Materials Research Proceedings 28 (2023) 93-100 https://doi.org/10.21741/9781644902479-11

Characterisation of the shape memory effect of PET polymer by FFF 3D printing

ERMOLAI Vasile[1,a *], SOVER Alexandru[1,b] and LANG Anette[1,c]

[1]Ansbach University of Applied Science, Faculty of Technology, Residenz str. 8, Ansbach, 91522, Germany

[a]vasile.ermolai@hs-anshach.de, [b]a.sover@hs-ansbach.de, [c]anette.lang@hs-ansbach.de

Keywords: Shape Memory Effect, Shape Recovery, PET, Fused Filament Fabrication

Abstract. In recent years the interest in finding new shape memory polymers has increased. Withal, fewer studies approached the use of regular materials such as polyethene terephthalate (PET), a widely available material. The research investigated the shape memory characteristics of regular PET 3D printed samples in two testing cycles. The recovery temperature was determined through dynamical mechanical, followed by tensile testing and heat treatment of the specimens. The results show PET has good shape memory properties, recording a slight increase in shape recovery during the second testing cycle without affecting the sample integrity. The thermal analysis of the recovered material shows that heat treatment time or/and temperature need to be improved to stabilise the PET material structure.

Introduction

Fused Filament Fabrication (FFF) is an extrusion-based additive manufacturing technology that uses filament shape thermoplastic materials as a feedstock. The material is heated until it reaches a viscous state and deposits layer-wise to build parts [1].

FFF disposes of a large variety of materials, including regular (polylactic acid), engineering grade (e.g., polycarbonate), or even high-performance polymers (e.g., polyether ether ketone) [2,3]. The technology is used for many applications, such as conceptual models, functional prototypes, tools and fixtures, replacement parts, biomedical applications, and others [4].

The design and production of a Shape Memory System (SMS) is another application of FFF. They are referred to as 4D printing because of their shape-changing behaviour over a period of time. These SMSs are compliant mechanisms that achieve motion based on a stimulus, in this case, shape change. This can be thermal, electromagnetic, light or pH-based and others [5-6].

The SMS is characterised by one or more shape-changing sequences and depends on the number of constituents. This way, the SMS can be divided into single, double, triple and multiple material mechanisms [5-7]. Regardless of the number of constituents, the working principle of polymeric SMS was classified into three mechanisms. The first is the dual-state mechanism. Here the permanent shape is memorised by the strong links of the polymeric chains (i.e., covalent bonds) and the temporary shape is maintained by the weak links (e.g., chain entanglements). The second is the dual-component mechanism. This one uses a more rigid component to "remember" the permanent shape and a softer one for the temporary shape. The third is the partial transition mechanism which uses a mixture of materials to provide the transition phases [8-10].

The shape memory properties are evaluated through the Fixity ratio (R_f) and Recovery ratio (R_r). Those are used to determine the Shape Memory Index (SMI) of the SMS [5-7] as follows:

$$R_f = \frac{\varepsilon_u}{\varepsilon_m} \quad (1)$$

$$R_r = \frac{\varepsilon_m - \varepsilon_p}{\varepsilon_m} \quad (2)$$

Content from this work may be used under the terms of the Creative Commons Attribution 3.0 license. Any further distribution of this work must maintain attribution to the author(s) and the title of the work, journal citation and DOI. Published under license by Materials Research Forum LLC.

$$SMI = R_f \times R_r \quad (3)$$

where ε_m is the specimen's elongation at 100%, ε_u is the elongation after release, and ε_p is the elongation after recovery.

For heat-sensitive SMSs, the permanent shape results after the part's manufacturing (i.e., after printing). Then the part is heated (at a temperature T_1 above the glass transition temperature) and deformed to a temporary shape. Then the permanent shape is recovered by heating the part at the same temperature, T_1 [5-7].

Polyethene terephthalate (PET) is a semicrystalline thermoplastic material and is characterised by both amorphous (i.e., transparent) and crystalline (i.e., opaque) phases [11,12]. It is widely used in the food industry for food and liquid containers [13,14] and as feedstock for additive manufacturing technologies such as FFF as a new or recycled material [15,16].

This work focused on evaluating the shape memory effect of specimens made of regular, neat PET. The sample deformation was made at room temperature in two testing cycles compared to the standard testing procedure. Shape memory specimens' cold deformation is documented in the literature [10,16,17]. The results show PET shape recovery is possible even after two cold deformation cycles.

Materials and Methods

The chosen material was a natural PET filament from BasicFil. This was printed as samples (i.e., type 5 of ASTM 638-14) using an Ultimaker 3 printer. Before printing, the material was dried in an oven at 65°C for four hours. The manufacturing instructions were generated using Cura 5.2.1 slicing tool using the main parameters described in Table 1.

Table 1. Printing process parameters.

1	Nozzle diameter (mm)	0.4	13	Print speed (mm/s)	30
2	Layer thickness (mm)	0.15	14	Travel speed (mm/s)	250
3	Extrusion width (mm)	0.4	15	Retraction distance (mm)	7
4	Number of walls	4	16	Retraction speed (mm/s)	35
5	Wall ordering	Outside to inside	17	Combing mode	Not in skin
6	Z seam position	Back left	18	Avoid printed at travel	Yes
7	Top/bottom layers	11	19	Z hop height (mm)	1.6
8	Top/bottom pattern	Lines	20	Regular fan speed (%)	15
9	Lines direction (°)	45/135	21	Maximum fan speed (%)	30
10	Extrusion temp. (°C)	245	22	Brim distance (mm)	0.1
11	Bed temp. (°C)	70	23	Brim width (mm)	3
12	Initial layer speed (mm/s)	15	24	Enclosure	Yes

The printing speed was controlled independently by each constructive element of the sample (e.g., walls, solid fill). The first layer and the brim were printed at a lover speed (i.e., 15 mm/s) to increase the adhesion with the build plate. To avoid the samples' deformation outside the gauge length, the walls closing was positioned in the samples' back left side (Fig. 1). This prevents closing contours from being placed by the slicing tool in the specimens' gauge or transition zones. Compared to the ASTM 638-14 standard specifications, the sample's thickness was increased to obtain an equal number of bottom and top layers. This way, the resulting thickness is 3.3 mm.

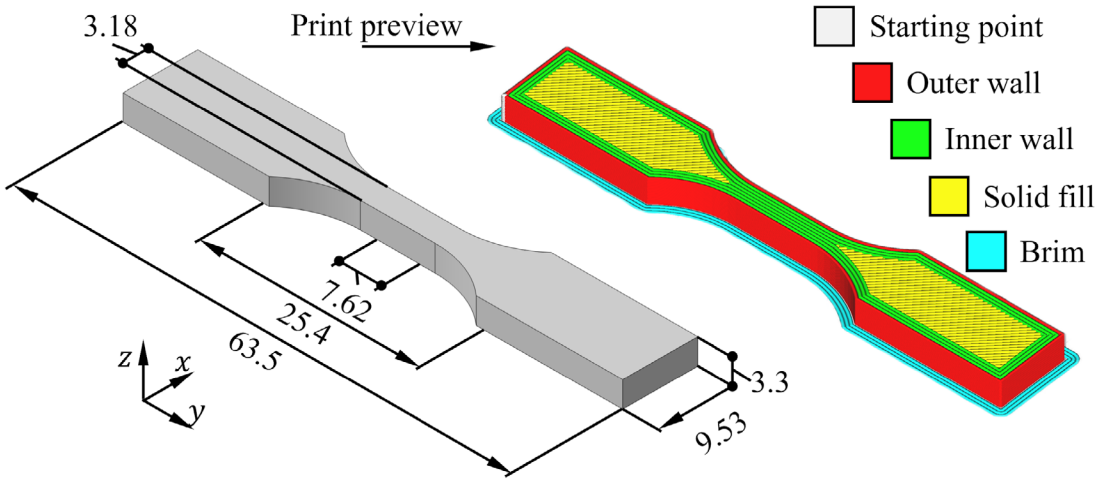

Fig. 1. CAD and printed specimen configuration.

The shape memory properties were determined by using the following steps:

1. Measurement of specimens' gauge length after marking;
2. Deformation at cold with 1 mm/min up to ε_m, the100% elongation;
3. Sample holding between clamping system for 5 minutes at ε_m;
4. Measurement of ε_u, the elongation after the release;
5. Heat treatment of the specimens in an oven at temperature T_1 for 5 minutes;
6. Measurement of ε_p, the recovery length.

The above-described steps were repeated for a second testing cycle, in which the new gouge length was the ε_p from the previous cycle. The testing cycles were performed with five replicates using an Instron 4411 universal testing machine with a load cell ok 5 kN. At the moment of testing, the laboratory had a temperature of 21°C and 52% moisture.

The heat treatment temperature T1 was established through dynamic mechanical analysis using TA instruments DMA 2980 equipment. Furthermore, to better understand PET's shape memory behaviour, musters of specimens' gauge zone at ε_u and ε_p were thermally analysed using Differential Scanning Calorimetry (DSC). An additional set of samples was prepared for the DSC measurements. The used equipment was a DSC 3+ from Mettler Toledo.

Results and Discussion

A dynamic mechanical analysis of the PET material was done to determine the recovery temperature for the shape memory characterisation. The test was performed in the multi-frequency method using a single cantilever bending at a frequency of 1 Hz. The temperature scans were performed at 2°C/min starting from 0 to 151.4°C when the material lost its properties. The glass transition temperature, T_g, occurs in a range, not on a single point or value. Based on the storage modulus onset, the T_g is at 76.22°C. It is the temperature at which this blend of PET starts to lose its mechanical properties. According to the loss modulus, the upper limit of the T_g range is 81.90°C. Usually, for shape memory polymers, the upper limit of the T_g is given by the tan δ modulus [10], because it is higher than the others. For the chosen blend of PET, the resulting tan δ modulus T_g value lies between the previously mentioned temperatures. All three diagrams are presented in Fig. 2. Based on these findings, a heat treatment temperature of 80°C was considered optimum for sample shape recovery.

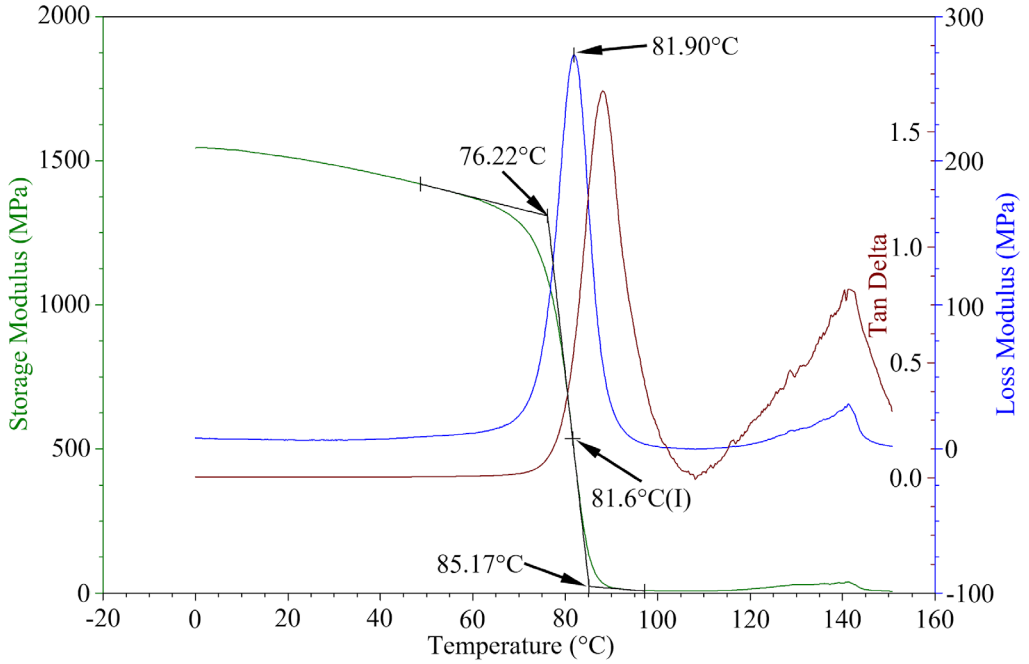

Fig. 2. Dynamical mechanical analysis of the chosen PET material.

All tested samples recorded similar deformation and shape recovery. In the first deformation-shape recovery cycle, the specimens presented a necking at the level of the gauge (see Fig. 3b). After the heat treatment at 80°C for 5 minutes, they partially recovered their shape (see Fig. 3c). Withal, in the second deformation-shape recovery cycle, the PET samples showed better shape memory effect compared to the previous one (see Fig. 3c and 3e).

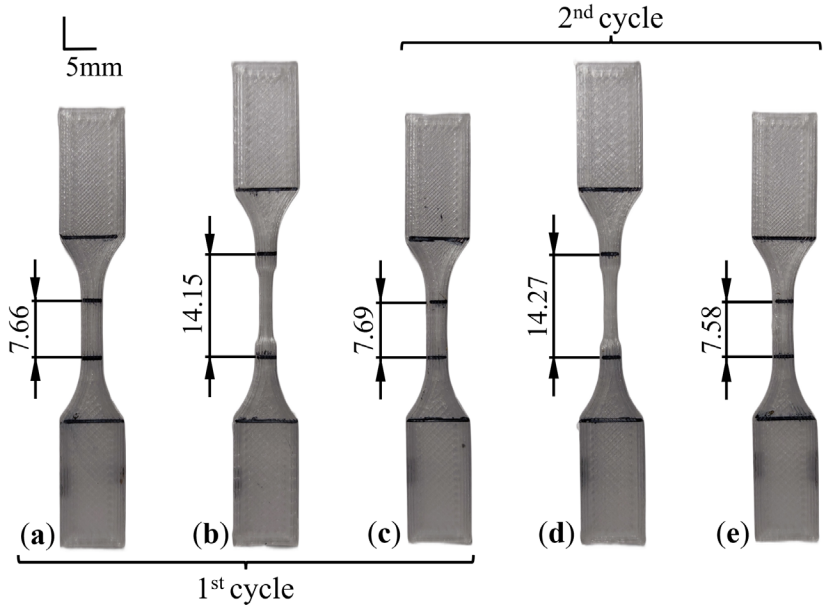

Fig. 3. Example of the PET samples at each step of the testing plan, with (a) initial, (b) first deformation, (c) first shape recovery, (d) second deformation, and (e) second shape recovery.

The fixity ratio, Rf, calculates the capacity of a material to memorise a shape by dividing ε_u at ε_m (Eq. 1). As presented in Fig. 4, the printed PET showed a good Rf in both of the testing cycles.

The samples recorded a slight increase in the second cycle compared to the first; the average fixity ratio is approximately 95%.

The recovery ratio, Rr, provides information regarding the materials' capability to recover their original shape when heated at temperature T_1. In the Fig. 4 plot, it is shown that in the first cycle, the PET samples showed an average recovery of 99.27%, and in the second cycle, it slightly increased to 100.19%. An example of the recovered parts is shown in Fig. 3.

The shape memory index gives information regarding materials' shape memory properties based on the previously presented ratios. Fig. 4 shows that PET samples averaged an SMI of 94.45% in the first testing cycle. The same samples gave an SMI average of 96.62% by performing a second set of trials. The resulting plot for each sample is presented in Fig. 4.

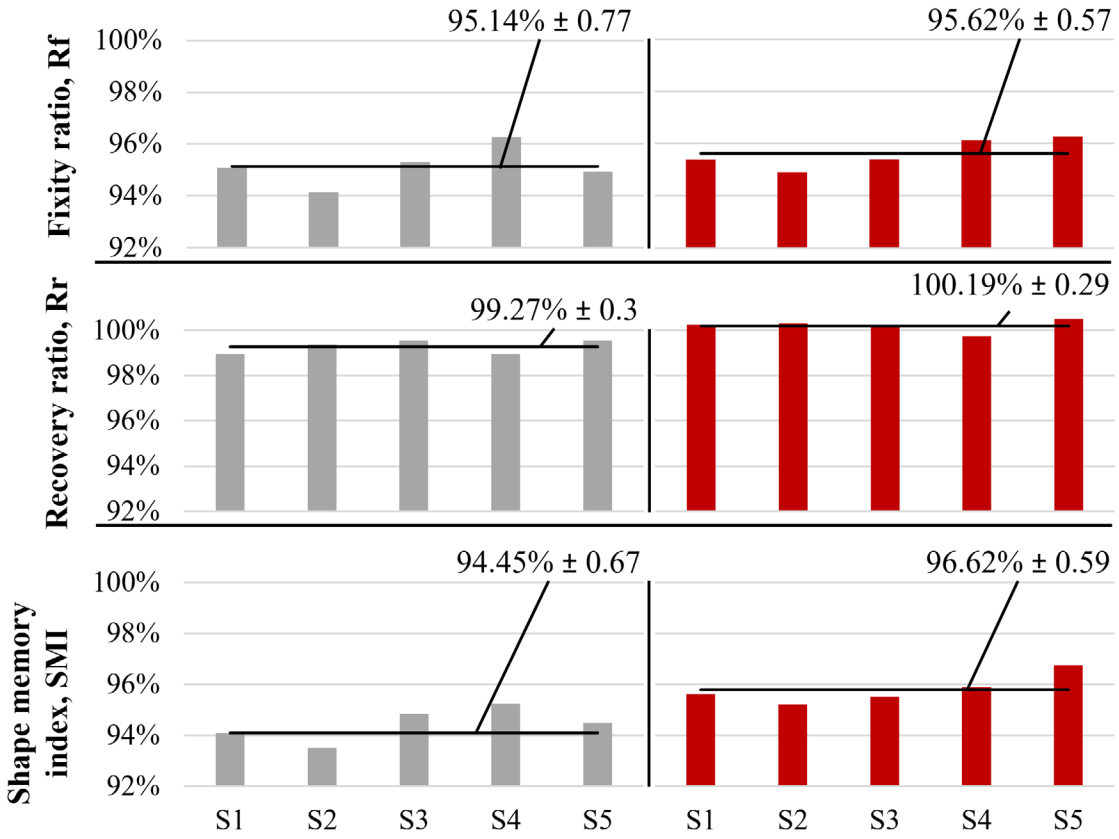

Fig. 4. Fixity ratio, recovery ratio and shape memory index of the tested samples.

To obtain more information regarding the shape memory properties increase in the second cycle, the stress-displacement plots of samples were analysed. Choosing the displacement instead of strain gives a more objective view as the specimens were elongated unevenly (see Fig. 5). At the first elongation, the samples showed similar peaks of the maximums stress with an average of 44.96±0.68 MPa and average stress at yield (at ε_m) of 28.33±0.28 MPa, in the second deformation cycle gave average maximum stress of 38.84±0.54 MPa and a 27.43±0.5 MPa yield average. By analysing the plots (see Fig. 5), it can be observed that the highest difference between the two cycles is at the maximum peak. For the rest of the tests, the results were comparable. As the samples are stretched, they follow the same pattern. First, a decrease of the load between 1 and 1.5 mm of displacement as the sample is necking. Then a slight but constant increase of the strength at yield.

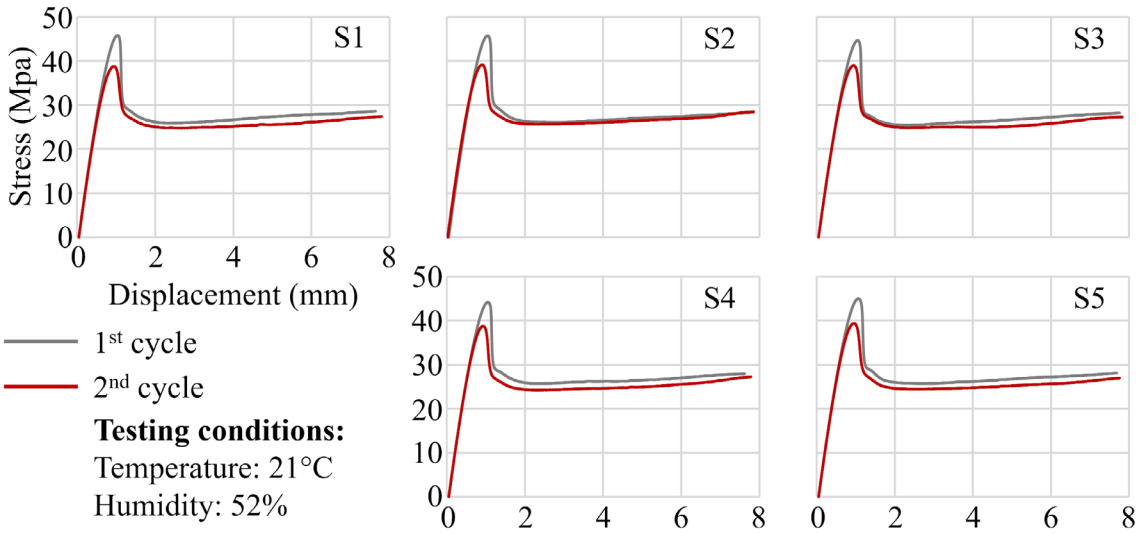

Fig. 5. Stress-displacement diagrams of the tested samples.

As the samples were elongated during the tensile test, the material situated in the gauge zone started to change its appearance from clear-transparent to an opaque white colour. This means that by stretching the sample, a change in crystallinity occurs in the material structure, from an initial amorphous to a semicrystalline state (Fig. 3). To find more information about the material behaviour, several DSC analyses were done on musters taken from the gauge zone. All studies were done by heating the material with 5 K/min from 20 to 100°C.

The first analysis was performed on a sample elongated at 100% (Fig. 3b). The result is presented in Fig. 6. It can be observed that between 40 and 60°C, the stretched material is taking energy, receiving a heat amount of 1.49 J/g. Because the material is deformed, it tends to regain its normal shape and consumes energy.

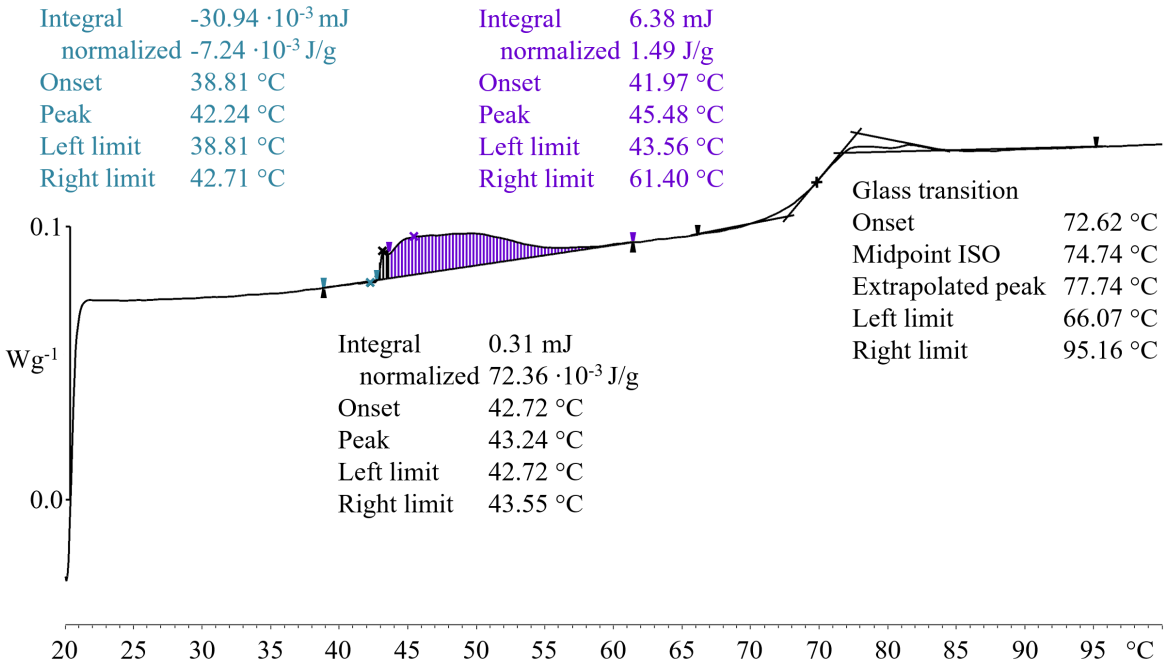

Fig. 6. DSC diagram of a first cycle elongated sample.

For the samples, after the first shape recovery, the DSC curves show that the heat-treated material is also absorbing energy between the 34 and 63°C range (see Fig. 7). However, the amount of energy required is less compared to the elongated materials. The material absorbed 0.72 J/g for the first sample, respectively 0.53 J/g for the second.

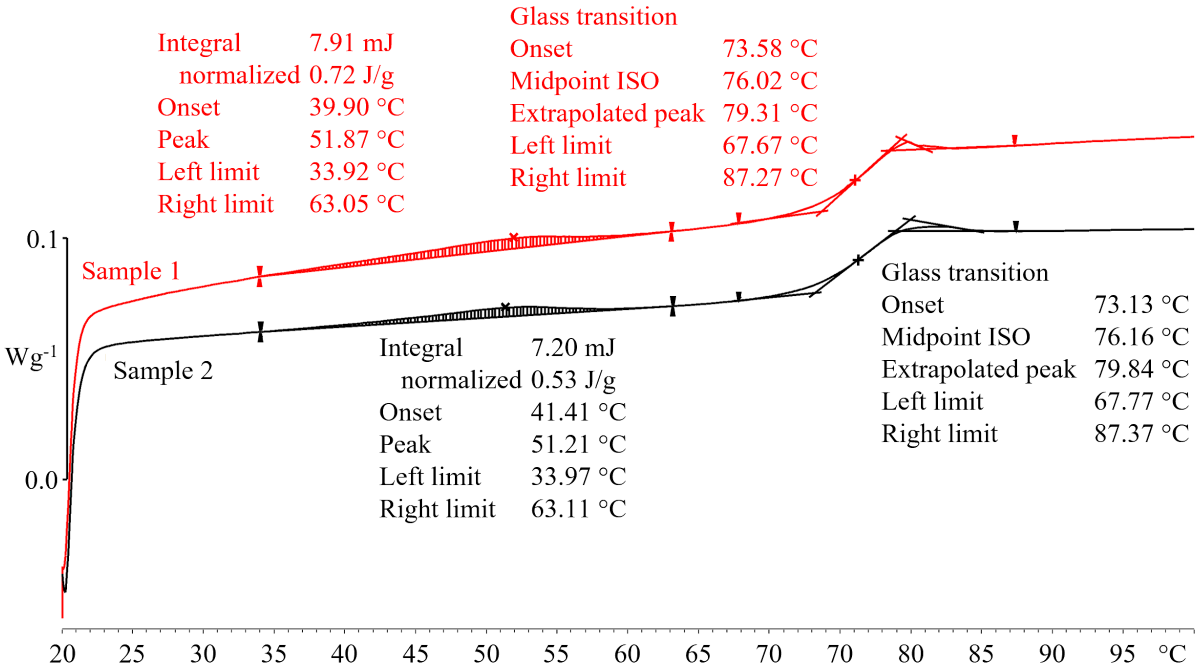

Fig. 7. DSC diagram of shape recovered samples.

Thermoplastics are characterised by covalent bonds of the polymeric chains and weaker bonds resulting from the chains' entanglements [11]. When stretched, the capacity of the chains to align with the load direction before breaking gives the maximum elongation. During the heat treatment, the polymeric chains tend to recover their natural state and reform the chains' entanglement. The DSC analysis of the heat-treated PET (Fig. 7) shows that the material required additional energy from the system. This suggests that an insufficient temperature or/and recovery time during the heat treatment possibly affected the polymeric chains' entanglement reformation. This aspect correlates with the decrease of the average maximum stress of ≈6 MPa during the tensile testing (Fig. 5). Further investigations are required for the structure of the elongated and heat-treated material to understand the PET shape memory properties better.

Summary

PET is a common thermoplastic material widely used in the food industry due to its good mechanical properties and processability. However, its shape memory properties were not thoroughly evaluated.

This study focused on evaluating the shape memory properties of PET 3D printed samples in two deformation-shape recovery cycles. Even if the samples' deformation was performed at cold, they obtained an average shape fixity of ≈95 in both testing cycles. On the other hand, the PET recovered its initial shape on an average of ≈99% testing cycle, respectively ≈100% in the second.

DSC analyses of the material heat-treated after elongation suggests that recovery temperature or/and time were not chosen accordingly to allow polymeric chains to entangle enough.

Further investigations are needed to better understand and control the PET material shape recovery during heat treatment.

References

[1] S. Singh, G. Singh, C. Prakash, S. Rama-Krishna, Current status and future directions of fused filament fabrication, J. Manuf. Process. 55 (2020) 288-306. https://doi.org/10.1016/j.jmapro.2020.04.049
[2] S. Kumar, R. Singh, T. Singh, A. Batish, Fused filament fabrication: A comprehensive review, J. Thermoplast. Compos. Mater. 36 (2020) 794-814. https://doi.org/10.1177/0892705720970629
[3] D. Popescu, A. Zapciu, C. Amza, F. Baciu, R. Marinescu, FDM process parameters influence the mechanical properties of polymer specimens: A review, Polym. Test. 69 (2018) 157-66. https://doi.org/10.1016/j.polymertesting.2018.05.020
[4] S. Hasanov, S. Alkunte, M. Rajeshirke, A. Gupta, O. Huseynov, I. Fidan, F. Alifui-Segbaya, A. Rennie, Review on Additive Manufacturing of Multi-Material Parts: Progress and Challenges, J. Manuf. Mater. Process. 6 (2022). https://doi.org/10.3390/jmmp6010004
[5] S. Valvez, P.N.B. Reis, L. Susmel, F. Berto, Fused Filament Fabrication-4D-Printed Shape Memory Polymers: A Review, Polym. 13 (2021) 701. https://doi.org/10.3390/polym13050701
[6] M. Rafiee, R.D. Farahani, D. Therriault, Multi-Material 3D and 4D Printing: A Survey, Adv. Sci. 7 (2020) 1902307. https://doi.org/10.1002/advs.201902307
[6] J. Carrell, G. Gruss, E. Gomez, Four-dimensional printing using fused-deposition modeling: a review, Rapid Prototyp. J. 26 (2020) 855-69. https://doi.org/10.1108/RPJ-12-2018-0305
[7] G. Scalet, Two-Way and Multiple-Way Shape Memory Polymers for Soft Robotics: An Overview, Actuators 9 (2020). https://doi.org/10.3390/act9010010
[8] J. Hu, Y. Zhu, H. Huang, J. Lu, Recent advances in shape–memory polymers: Structure, mechanism, functionality, modeling and applications, Prog. Polym. Sci. 37 (2012) 1720-1763. https://doi.org/10.1016/j.progpolymsci.2012.06.001
[9] M.C. Biswas, S. Chakraborty, A. Bhattachar-Jee, Z. Mohammed, 4D Printing of Shape Memory Materials for Textiles: Mechanism, Mathematical Modeling, and Challenges, Adv. Funct. Mater. 31 (2021) 2100257. https://doi.org/10.1002/adfm.202100257
[10] P.A. Quiñonez, L. Ugarte-Sanchez, D. Bermudez, P. Chinolla, R. Dueck, T.J. Cavender-Word, D.A Roberson, Design of Shape Memory Thermoplastic Material Systems for FDM-Type Additive Manufacturing, Materials 14 (2021) 4254. https://doi.org/10.3390/ma14154254
[11] G.W. Ehrenstein, Structure of Polymeric Materials, In: Polymeric materials, Hanser, Ohio, 2001, pp. 61-141. https://doi.org/10.3139/9783446434134.004
[12] A. Bartolotta, G. Di Marco, F. Farsaci, M. Lanza, M. Pieruccini, DSC and DMTA study of annealed cold-drawn PET: a three-phase model interpretation, Polym. 44 (2003) 5771-5777. https://doi.org/10.1016/S0032-3861(03)00589-5
[13] R. Nisticò, Polyethylene terephthalate (PET) in the packaging industry, Polym. Test. 90 (2020) 106707. https://doi.org/10.1016/j.polymertesting.2020.106707
[14] P. Benyathiar, P. Kumar, G. Carpenter, J. Brace, D.K. Mishra, Polyethylene Terephthalate (PET) Bottle-to-Bottle Recycling for the Beverage Industry: A Review, Polym. 14 (2022) 2366. https://doi.org/10.3390/polym14122366
[15] D. Fico, D. Rizzo, R. Casciaro R, C. Esposito Corcione, A Review of Polymer-Based Materials for Fused Filament Fabrication (FFF): Focus on Sustainability and Recycled Materials, Polym. 14 (2022) 465. https://doi.org/10.3390/polym14030465
[16] B. Pricop, Ș.D. Sava, N.M. Lohan, L.G. Bujoreanu, DMA Investigation of the Factors Influencing the Glass Transition in 3D Printed Specimens of Shape Memory Recycled PET, Polym. 14 (2022) 2248. https://doi.org/10.3390/polym14112248
[17] V. Ermolai, A. Sover, G. Nagîț, A.I. Irimia, 2022, Shape recovery properties of PET-based 3D printed samples, presented at Innovative Manufacturing Engineering & Energy (IManEE), Iași, 17-19 November.